

## Supporting Information

### One-step green synthesis of Cu<sub>2</sub>O/CuO@rGO composites for ppt level detection of NO<sub>2</sub> at room temperature

Jinjuan Li,<sup>a#</sup> Jing Hu,<sup>\*a,b#</sup> Nan Li,<sup>a</sup> Miao Cheng,<sup>a</sup> Tao Wei,<sup>a</sup> Qianqian Liu,<sup>a</sup> Ruirui Wang,<sup>a</sup> Wanfei Li,<sup>a</sup> Yun Ling,<sup>a,c</sup> Yafei Zhang<sup>d</sup> and Bo Liu<sup>\*a</sup>

- a. *Suzhou Key Laboratory for Nanophotonic and Nanoelectronic Materials and Its Devices, School of Materials Science and Engineering, Suzhou University of Science and Technology, Suzhou 215009, Jiangsu Province, China.*
- b. *State Key Laboratories of Transducer Technology, Shanghai 200050, PR China.*
- c. *School of electronic & information engineering, Suzhou University of Science and Technology, Suzhou 215009, Jiangsu Province, China.*
- d. *Key Laboratory for Thin Film and Microfabrication of the Ministry of Education, Department of Micro/Nano Electronics, School of Electronics, Information and Electrical Engineering, Shanghai Jiao Tong University, Shanghai 200240, PR China.*

\* Corresponding author, Tel:+86-0512-68416733; Fax: +86-0512-68416733; Email: hujlina@usts.edu.cn; chengmiao@usts.edu.cn; liubo@mail.usts.edu.cn.

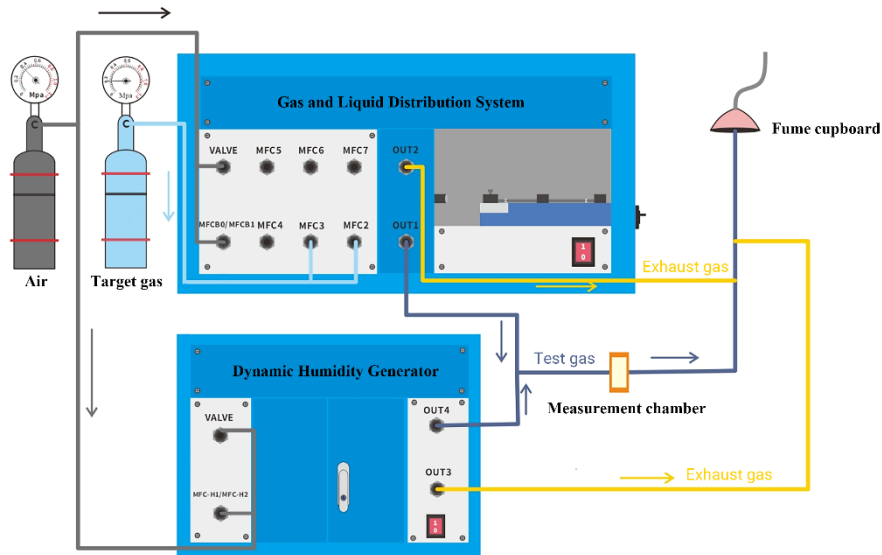


**Fig. S1** Schematic diagram of dynamic gas sensitivity test system.

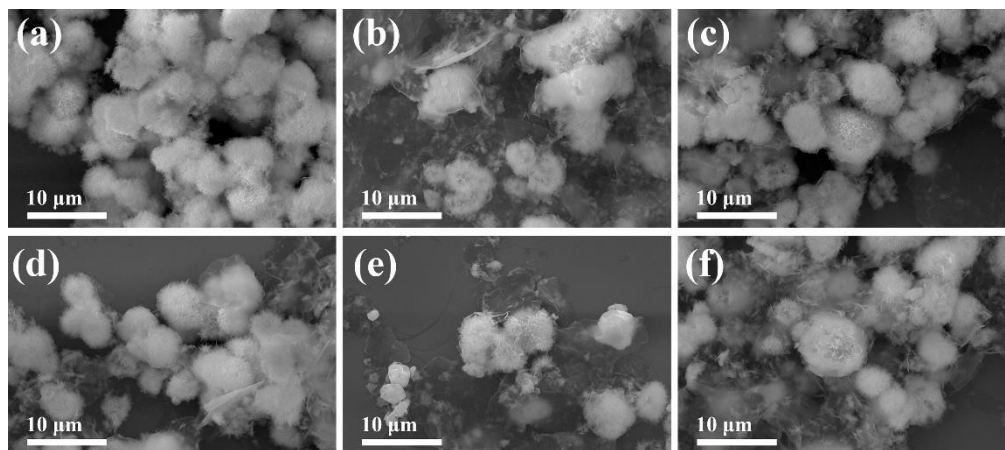


**Fig. S2** FE-SEM images of (a) 550Cu<sub>2</sub>O/CuO-5; (b) 150Cu<sub>2</sub>O/CuO@rGO-5; (c) 300Cu<sub>2</sub>O/CuO@rGO-5; (d) 450Cu<sub>2</sub>O/CuO@rGO-5; (e) 550Cu<sub>2</sub>O/CuO@rGO-5 and (f) 650Cu<sub>2</sub>O/CuO@rGO-5.

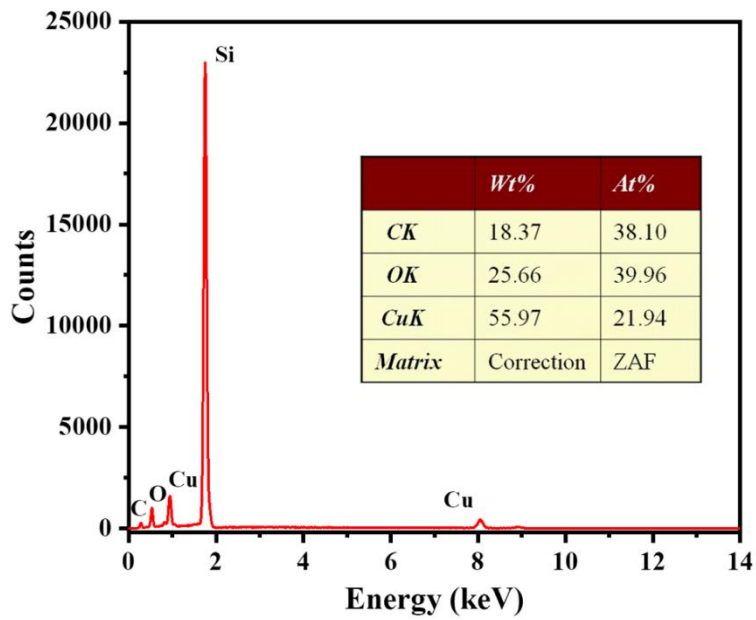


**Fig. S3.** EDX analysis of the 550Cu<sub>2</sub>O/CuO@rGO-5.

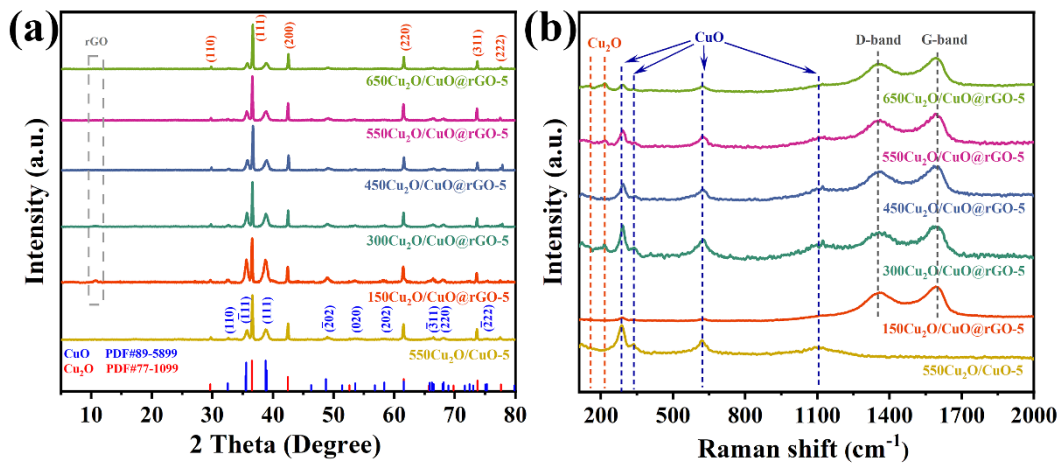


**Fig. S4.** (a) XRD and (b) Raman spectra of Cu<sub>2</sub>O/CuO@rGO-5 composites with different Cu<sub>2</sub>O additions.

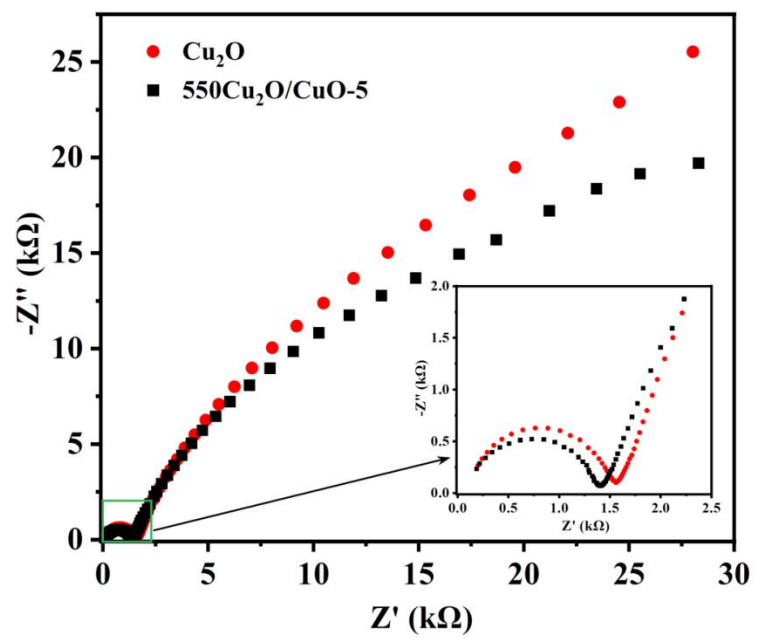


**Fig. S5.** Electrochemical impedance spectroscopy (Nyquist diagram) of pure  $\text{Cu}_2\text{O}$  and  $550\text{Cu}_2\text{O}/\text{CuO-5}$  materials.

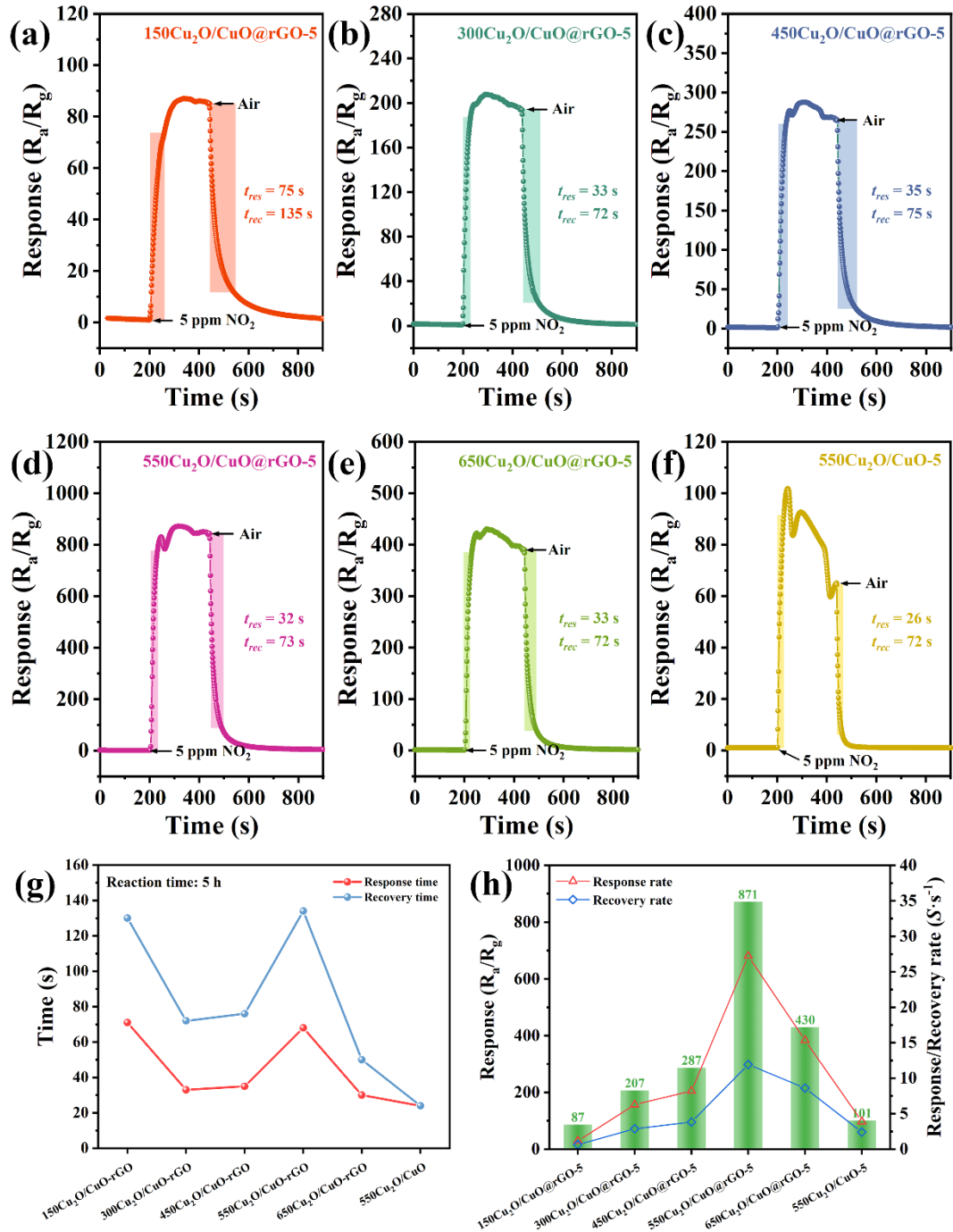


**Fig. S6.** Dynamic response-recovery curve of (a-e)  $\text{Cu}_2\text{O}/\text{CuO}@\text{rGO-5}$  sensors with different  $\text{Cu}_2\text{O}$  additions and (f) 550Cu<sub>2</sub>O/CuO sensor to 5 ppm  $\text{NO}_2$  at RT; (g) response/recovery time of  $\text{Cu}_2\text{O}/\text{CuO}@\text{rGO-5}$  sensors with different Cu<sub>2</sub>O additions and 550Cu<sub>2</sub>O/CuO sensor with different reaction time to 5 ppm  $\text{NO}_2$  at RT; (h) response and response/recovery rate of  $\text{Cu}_2\text{O}/\text{CuO}@\text{rGO-5}$  sensors with different Cu<sub>2</sub>O additions and 550Cu<sub>2</sub>O/CuO sensor with different reaction time to 5 ppm  $\text{NO}_2$  at RT.

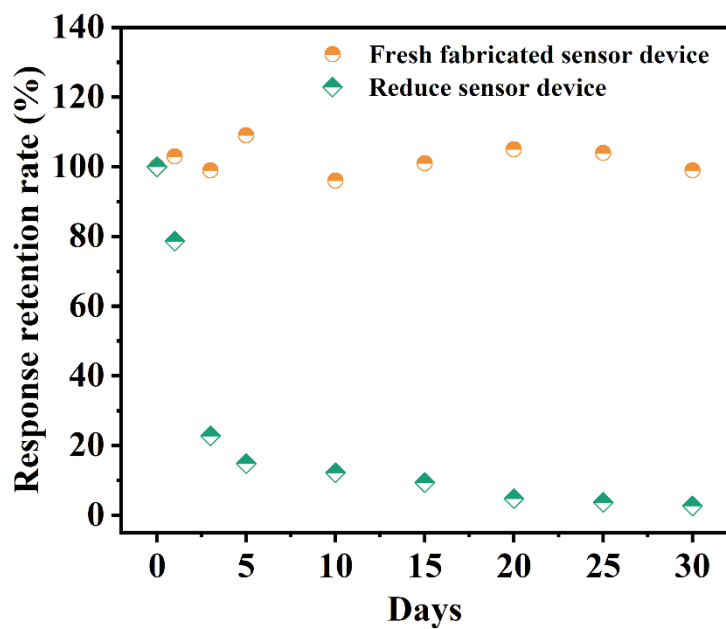


**Fig. S7.** The stability evaluation of the as-prepared 550Cu<sub>2</sub>O/CuO@rGO-5 sensor within one month.

## The evolution mechanism of the Cu<sub>2</sub>O/CuO materials

The chemical equation of CuO obtained from Cu<sub>2</sub>O is shown in Eq. 1-2. The excess OH<sup>-</sup> in the solution together with O<sub>2</sub> etch the surface of Cu<sub>2</sub>O and form [Cu(OH)<sub>4</sub>]<sup>2-</sup> (Eq. 1). However, because [Cu(OH)<sub>4</sub>]<sup>2-</sup> is unstable, it will decompose into CuO and H<sub>2</sub>O (Eq. 2). At the same time, it self-assembles around the Cu<sub>2</sub>O to form urchin-like Cu<sub>2</sub>O/CuO spheres. Similarly, we have added the relevant description in the revised version.



## LOD

The sensor noise can be calculated by the change of the relative response of the sensor in the baseline. Ten consecutive data collected before exposure to NO<sub>2</sub> gas were averaged, and the standard deviation (S) calculated using the root mean square deviation (RMSD)<sup>1</sup> formula was 0.00022.

$$\text{RMS}_{\text{noise}} = \sqrt{\frac{S^2}{N}} \#(3)$$

where N is the number of data points. The RMS<sub>noise</sub> is calculated according to the above Eq. 3 to be 0.000156. According to the definition of detection limit (three times the standard deviation of noise). The slope is 0.00227 from Fig. 8d, so that

$$\text{LOD} = 3 \times \frac{\text{RMS}_{\text{noise}}}{\text{slope}} = 0.0906 \text{ ppb} = 90.6 \text{ ppt} \#(4)$$

**Table S1.** The peak intensity ratio between Cu<sub>2</sub>O and CuO and between D band and G band in Cu<sub>2</sub>O/CuO@rGO-5 composites varies with the amount of Cu<sub>2</sub>O added.

Sample at different Cu <sub>2</sub> O addition amount (mg)	GO	150	300	450	550	650
I <sub>Cu<sub>2</sub>O (111)</sub> /I <sub>CuO (111)</sub>	—	1:0.518	1:0.293	1:0.231	1:0.233	1:0.211
I <sub>D</sub> /I <sub>G</sub>	1.28	1.16	0.99	0.99	0.98	0.92

**Table S2.** NO<sub>2</sub> response of Cu<sub>x</sub>O-based and rGO-based sensors in different work and the gas sensor in this work.

Material	Synthesis method/temperature	Work Temperature	Response	$\tau_{\text{res}}/\tau_{\text{rec}}$	LOD
Cu <sub>2</sub> O-CuO <sup>2</sup>	One -step/180 °C	187 °C	10.2 (1 ppm)	35/47*	—
CuO-Co <sub>3</sub> O <sub>4</sub> <sup>3</sup>	Multi-step/450 °C	160 °C	37.86% (10 ppm)	158/738*	—
CuO/ZnO <sup>4</sup>	Multi-step/400 °C	RT (30 °C)	337% (5 ppm)	18/32	155 ppb
BiVO <sub>4</sub> /Cu <sub>2</sub> O/rGO <sup>5</sup>	Multi-step/180 °C	60 °C	8.1 (1 ppm)	51.3/87.5*	100 ppb
Cu <sub>2</sub> O/rGO <sup>6</sup>	Multi-step/200 °C	RT	67.80% (2 ppm)	~440/490	82 ppb
CuO/rGO <sup>7</sup>	Multi-step/80 °C	RT (23 °C)	400.80% (5 ppm)	6.8/55.1*	50 ppb
CuO/rGO <sup>8</sup>	One-step/25 °C	RT	74395.2 (50 ppm)	30/270	100 ppb
CuO/rGO <sup>9</sup>	One-step/180 °C	RT	30% (50 ppm)	Irreversible	150 ppb
rGO/Cu <sub>2</sub> O <sup>10</sup>	Multi-step/100 °C	RT	5.2 (1 ppm)	29.2/76.8	32 ppb
<b>550Cu<sub>2</sub>O/CuO@rGO-5<sup>This work</sup></b>	One-step/25 °C	<b>RT (25 °C)</b>	<b>871 (5 ppm)</b>	<b>35/73</b>	<b>90.6 ppt</b>

\* Representing that  $\tau_{\text{res}}/\tau_{\text{rec}}$  is defined in the literature as 90% of the change in resistance value.

## Reference

1. V. Dua, S. P. Surwade, S. Ammu, S. R. Agnihotra, S. Jain, K. E. Roberts, S. Park, R. S. Ruoff and S. K. Manohar, *Angew. Chem. Int. Ed. Engl.*, 2010, **49**, 2154-2157.
2. N. Wang, W. Tao, X. Q. Gong, L. P. Zhao, T. S. Wang, L. J. Zhao, F. M. Liu, X. M. Liu, P. Sun and G. Y. Lu, *Sens. Actuators, B*, 2022, **362**, 131803.
3. H. R. Fang, S. Li, H. M. Zhao, J. Deng, D. Wang and J. Li, *Sens. Actuators, B*, 2022, **352**, 131068.
4. A. Govind, P. Bharathi, M. K. Mohan, J. Archana, S. Harish and M. Navaneethan, *J. Environ. Chem. Eng.*, 2023, **11**, 110056.
5. Q. Q. Li, N. Han, K. W. Zhang, S. L. Bai, J. Guo, R. X. Luo, D. Q. Li and A. F. Chen, *Sens. Actuators, B*, 2020, **320**, 128284.
6. S. Deng, V. Tjoa, H. M. Fan, H. R. Tan, D. C. Sayle, M. Olivo, S. Mhaisalkar, J. Wei and C. H. Sow, *J. Am. Chem. Soc.*, 2012, **134**, 4905-4917.
7. H. N. Bai, H. Guo, J. Wang, Y. Dong, B. Liu, Z. L. Xie, F. Q. Guo, D. J. Chen, R. Zhang and Y. D. Zheng, *Sens. Actuators, B*, 2021, **337**, 129783.
8. J. Hu, M. Cheng, T. Wei, Q. Q. Liu, W. F. Li, Y. Ling, Y. F. Zhang and B. Liu, *Mater. Sci. Semicond. Process.*, 2022, **138**, 106289.
9. Z. Bo, X. Wei, X. Z. Guo, H. C. Yang, S. Mao, J. H. Yan and K. F. Cen, *Chem. Phys. Lett.*, 2020, **750**, 137485.
10. J. L. Pan, W. Q. Li, L. Quan, N. Han, S. L. Bai, R. X. Luo, Y. J. Feng, D. Q. Li and A. F. Chen, *Ind. Eng. Chem. Res.*, 2018, **57**, 10086-10094.